Available online at www.sciencedirect.com
SCIENCE DIRECT®
ELSEVIER
Journal of Computational Physics 194 (2004) 329–343
JOURNAL OF COMPUTATIONAL PHYSICS
www.elsevier.com/locate/jcp

On the application of congruent upwind discretizations for large eddy simulations

Andrea Aprovitola, Filippo Maria Denaro *

Dipartimento di Ingegneria Aerospaziale e Meccanica, Seconda Università di Napoli, via Roma 29, Aversa 81031, Italy

Received 10 February 2003; received in revised form 24 July 2003; accepted 15 September 2003

Abstract

Upwind schemes were judged inappropriate for performing accurate large eddy simulations of turbulent flow owing to the artificial dissipation that is present at high wavenumbers of the energy content. Such a conclusion has been drawn also from some results obtained by adopting Finite Difference schemes. The present paper illustrates the performances of some new Finite Volume upwind discretization of the convective terms in the case of the 1-D Burgers model equation while studying the effects of numerical discretization on several Sub-Grid Scales turbulence models, starting from the classical static and dynamic eddy viscosity models through the recent deconvolution-based ones. Basing on previously published papers, large eddy simulations along with a deconvolution-based procedure for de-filtering the evolving variable, have been originally developed and applied. It will be shown how the coherent application of the procedure allows us to develop high-order accurate Finite Volume upwind schemes, which maintain a good spectral resolution in the entire range of resolved scale. Such schemes can be candidate for performing accurate simulations of real turbulence.

AMS: 65C20; 65M99; 76D05

Keywords: Finite volumes method; Conservative upwind Schemes; Large eddy simulation

1. Introduction

Despite of some successful Direct Numerical Simulation (DNS) of turbulence, e.g., see [1], upwind schemes are considered inappropriate for performing Large Eddy Simulation (LES), since they introduce a dissipative numerical error, mainly acting at high resolved wavenumbers, which can contaminate the modelled Sub-Grid Scales (SGS) stress [2]. Such a conclusion is derived from inspection of the local truncation error as well as from the fact that when the derivatives are discretized over non-symmetric

* Corresponding author. Fax: +39-081-5010264.
E-mail address: denaro@unina.it (F.M. Denaro).

doi:10.1016/j.jcp.2003.09.027

stencils they present modified wavenumbers with a non-vanishing imaginary part. This feature is simply illustrated by considering the linear transport equation

$$\frac{\partial \phi}{\partial t} + c\frac{\partial \phi}{\partial x} = 0,$$

being c a positive constant, with some upwind-based Finite Difference (FD) spatial discretization. For a single Fourier component, it can be shown that the exact solution of the semi-discretized equation is

$$\phi(x,t) = A_q \mathrm{e}^{-\mathrm{Im}(k_{\mathrm{eff}})ct/k_q} \mathrm{e}^{\mathrm{i}k_q[x-\mathrm{Re}(k_{\mathrm{eff}})ct/k_q]},$$

being $k_q = 2\pi q/L$ the wavenumber, k_{eff} the modified wavenumber, $\mathrm{Re}(k_{\mathrm{eff}})$ and $\mathrm{Im}(k_{\mathrm{eff}})$ its real and imaginary part, respectively. Each type of upwind discretization generates some expression $k_{\mathrm{eff}}/k_q \neq 1$ therefore, with respect to the exact solution of the differential equation, i.e., $\phi(x,t) = A_q \mathrm{e}^{\mathrm{i}k_q(x-ct)}$, the real part causes a *dispersion error*, the imaginary part a *diffusion error*. More specific analyses reveal [2] that a good resolution is obtained only up to a half of the resolved range whereas the higher part is contaminated by diffusion and dispersive errors.

In contrast to upwind discretization, FD central schemes characterizes only a real modified wavenumber thus, they highlight only a corresponding dispersion error that is responsible of the well-known energy pile-up phenomenon. Such behaviour motivated the preference of central schemes over upwind ones for performing LES. On the other hand, the simulation of wall-bounded flows requires the adoption of non-uniform grids, i.e., non-symmetric stencils, for which, unfortunately, also central schemes involve diffusion errors, too. It is consequent that asymmetric discretization deserves extreme care.

As a matter of fact, while some attention was devoted to analyse high order FD upwind schemes it appears that the analysis of Finite Volume (FV) discretization is less focused. FV methods are based on to the discretization of the integral form of conservation laws therefore these methods guarantee, a priori, the discrete conservation of the balanced variable. This fact is particularly important since it is known that discrete conservation property ensures the correct waves velocity propagation. Correct shock-waves propagation in inviscid flows is the most intuitive case wherein such property is fundamental but turbulent flows represent themselves a case of strong interaction between waves at high wavenumber that must be correctly described. Of course, the integral form of the transport equations is also mathematically necessary for inviscid flows when singularities can appear. Furthermore, a volume integral in FV represents a natural link with discrete spatial filtering (the so-called *top-hat* filtering) in LES. This issue has been introduced and discussed in [3] wherein a deconvolution-based procedure has driven to develop a high order filtering procedure and to express several discretization on uniform grids, both centred and up-winded. The local truncation errors for those high order conservative schemes were reported along with the corresponding spectral distribution errors. Moreover, a theoretical analysis for the 1-D Burgers model equation showed that the SGS term to be modelled in the deconvolved equation gets smaller importance by increasing the deconvolution order. That theoretical analysis onto the deconvolved field was only limited at a fixed time while a preliminary simulation of the 3-D backward-facing step flow was performed for a no-model LES with third order accurate upwind discretization. Then, the deconvolution-based FV approach has been recently theoretically extended to a central fourth order accurate discretization on non-uniform grids and applied for simulating a 2-D evolving mixing layer [4].

The present contribution, compared to the previous works, concerns both the study of the performances of several FV upwind discretization for a time evolving field and the study of the effects of several SGS models, starting from the classical static and dynamic eddy viscosity models through the recent deconvolution based ones, e.g. see [5–8], that are naturally linked to our procedure. In order for the effective performances of such models to be explored, upwind and central discretizations of the convective term in the case of the 1-D Burgers equation are compared in LES framework. As assessment, a well-resolved DNS is also developed. It will be shown how the coherent application of the procedure allows us to develop high-order accurate FV upwind schemes, which maintain a good spectral resolution in the entire range of resolved scale. The Burgers equation has been considered a useful simplified model equation for studying turbulence in virtue of its non-linear character [9,10]. As a matter of fact, this simple turbulence model gained new consideration in the modern LES research as demonstrated by some recent publications, e.g., [8,11,12]. This is because the non linear term is quadratic as in the Navier–Stokes equations and the Burgers turbulence exhibits an inertial range wherein low wavenumber flow components transfer energy to the higher ones until to dissipate in the dissipative range, similar to that of real turbulence. Dynamics of the small scales in Burgers turbulence is different from that of the Navier–Stokes because small flow scales are shocks of thickness proportional to the viscosity [9] and are essentially not stochastic [11]. Moreover, some other different behaviour can appear between Burgers and real turbulence [11] therefore some results can not necessarily be extended to real flows. Of course, the 1-D Burgers model can not allow us to provide a full judgment of a well described turbulence field, for example because vorticity dynamics is not present. However, the Burgers problem allows more complex SGS models to be evaluated than was possible in three-dimensional turbulence and, once highlighted the differences, some insights can be gained and a guideline for simulating 3-D LES can be pursued.

2. Burgers equation and finite volume methodology

Consider in $[0, L[\times[0, \infty[$, with periodic boundary conditions, the equation

$$\frac{\partial u}{\partial t} + \frac{\partial f(u)}{\partial x} = 0, \tag{1}$$

with $f = (u^2/2) - \nu(\partial u/\partial x)$ and assigned initial condition $u(x,0) = u_0(x)$ having a vanishing mean value. For a periodic function u one has its Fourier representation $u(x,t) = \sum_q \hat{u}_q(t)\mathrm{e}^{\mathrm{i}k_q x}$ and its energy content $E(k_q,t) = |\hat{u}_q(t)|^2$. As initial condition, the prescribed energy spectrum has the form:

$$E_{q0} \equiv E(k_q, 0) = A\sigma^5 k_q^4 \mathrm{e}^{-\sigma^2 k_q^2/2} \tag{2}$$

being the constant $A = U_0^2/(3\sqrt{2\pi})$ with $U_0^2 \equiv \langle u_0^2(x)\rangle$ the mean kinetic energy at $t = 0$. The energy spectrum E_{q0} has a maximum value at $(k_q)_{\max} = 2/\sigma$ while resulting $\int_0^\infty E_{q0}\,\mathrm{d}k_q = U_0^2/2$. For the present study, the prescribed numerical values are $\sigma = 0.05L/2\pi$ for $(k_q)_{\max} = 80\pi/L$. The initial velocity field is obtained by means of the Wiener process over $N_c = 32$ samples, as it is explained in details in [13]. The averaged spectrum, obtained with the 32 samples at the initial time, is reported in Fig. 1(a).

Starting from this initial condition, owing to the non-linearity (the non-linear term is quadratic as in the Navier–Stokes equation), the velocity field develops higher gradient, tending to form shock-waves, until the viscous term becomes predominant over the smallest scales and guarantees the solution to remain regular. In absence of a forcing term, the diffusion will act to dissipate the gradients until the rest is reached. When the velocity field develops, the energy spectrum shows an inertial sub-range having a −2 slope, according to what analysed in [9–13]. In Fourier space one can see, during the initial developing and for sufficiently small molecular viscosity, an enlargement of the energy spectrum frequencies range, without a noticeable energy decaying, similarly to an inviscid transient. Only successively the dissipative effects become manifest, decreasing the energy content and increasing the characteristic length scales of the dissipative range.

Now, let us briefly introduce the deconvolution-based FV procedure, detailed in [3,4]. By integrating Eq. (1) over an elementary volume of length Δ one has

$$\frac{\partial \overline{u}}{\partial t} + \frac{1}{\Delta}\left| f(u)\right|_{x-\Delta/2}^{x+\Delta/2} = 0$$

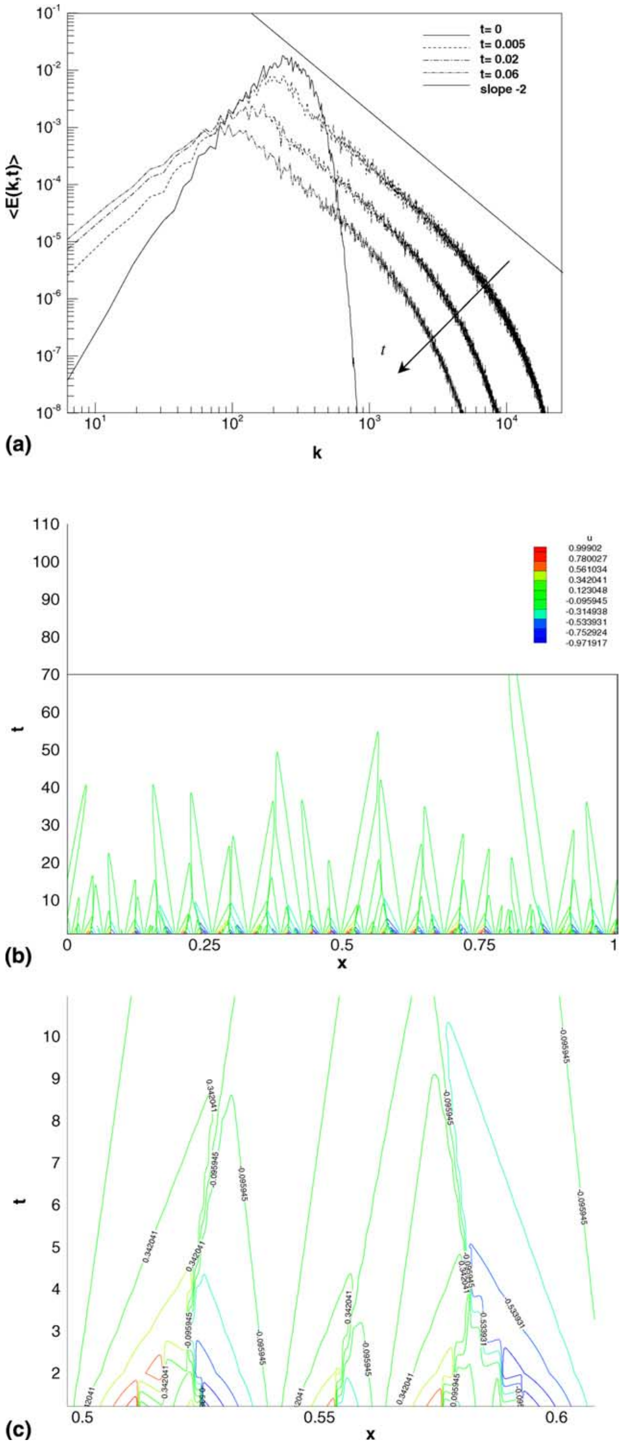

Fig. 1. (a) DNS. Energy spectra for $t = 0$, 0.006, 0.02, 0.08. (b) DNS. Velocity isolines in the x, t plane. (c) DNS. Zoom of the velocity isolines in the x, t plane.

having defined the volume averaged (nothing else that the *top-hat* filtered) variable

$$\overline{u}(x,t) = \frac{1}{\Delta}\int_{x-\Delta/2}^{x+\Delta/2} u(\xi,t)\,\mathrm{d}\xi \equiv G * u.$$

It is well known that the top-hat filter kernel G has no exact inverse therefore only an approximate inversion of the relation above can be performed. Based on a Taylor series approximation, integrated over the elementary volume, one transforms [3] the entire equation by applying to both terms the approximate deconvolution operator of order m, say $A^{(m)}$, as

$$\frac{\partial \tilde{u}}{\partial t} = \frac{1}{\Delta}\left[A^{(m)}\left(-\frac{\tilde{u}^2}{2} - \frac{\tau}{2}\right)\right]_{x-\Delta/2}^{x+\Delta/2} + \frac{\partial}{\partial x}\left(\nu\frac{\partial \tilde{u}}{\partial x}\right), \tag{3}$$

being

$$\tilde{u}(x) = \frac{1}{\Delta}\int_{x-\Delta/2}^{x+\Delta/2} A^{(m)} u\,\mathrm{d}\xi \equiv G_m^{-1} * \overline{u}$$

the mth order deconvolved velocity field,

$$A^{(m)} = I - \frac{\Delta^2}{24}\frac{\partial^2}{\partial x^2} + \frac{7\Delta^4}{5760}\frac{\partial^4}{\partial x^4} + \cdots$$

and having defined the exact SGS stress $\tau = u^2 - \tilde{u}^2$. The Eq. (3) represents the Burgers equation for the velocity $\tilde{u}$. Let us highlight that in order for Eq. (3) to be correct, a uniform filter width is necessary for ensuring commutation with $A^{(m)}$. In case of non-uniform width, the deconvolution-based FV equation (3) is modified, according to [4], by solving an implicit equation with the inverse of $A^{(m)}$ applied to the right-hand side. This way, it is not necessary to solve the LES equation with the explicit computation of the commutation terms.

Spectral resolution of the deconvolved field $\tilde{u}$ is illustrated in [3,4] wherein it is clearly demonstrated that the highest resolved wavenumbers are better represented then those of the top-hat variable $\overline{u}$. An important consequence of this fact is that the discrete filter implicated in the present method, is a symmetric Padè-type filter, its transfer function being shown [3,4] to result

$$\hat{G}(\eta) = \left(\frac{41}{48} + \frac{\cos\eta}{6} - \frac{\cos 2\eta}{48}\right)\Big/\left(\frac{43}{48} + \frac{\cos\eta}{9} - \frac{\cos 2\eta}{144}\right),$$

with $\eta = k_q h$. Of course, the transfer function acts only up to the Nyquist wavenumber π/h, corresponding to the numerical grid size $h = x_j - x_{j-1}$. This fact justifies the good spectral resolution achieved by $\tilde{u}$ and the hope to apply the formulation in LES approach.

The proposed FV schemes are obtained by prescribing the order $(m+1)$ of the de-filtering operator $A^{(m)}$ and a Lagrangian polynomial of g degree for the convective flux function to be computed over an upwinded stencil whereas, for consistence reasons, it is chosen $m = g = 2, 4$. For example, assuming a positive velocity, for $g = 2$ (third order upwind scheme, denoted as UW3) one has the stencil $(j-2,\ldots,j+1)$ while for $g = 4$ one can choose either the full upwind $(j-4,\ldots,j+1)$ or the upwind-biased $(j-3,\ldots,j+2)$ stencils (fifth order upwind schemes denoted as UW5 and UWB5, respectively). It is worth highlighting that in our procedure the uniform mesh size, which is used for flux reconstruction, could be made distinct from the volume measure so that $h < \Delta$. However, though it is expect to enhance the accuracy, such procedure has not been yet implemented and $h = \Delta$ is used.

For the sake of completeness, a fifth order FD upwind-biased scheme (UWB5NC) is also adopted, while considering the convection term in non-conservative form. Note, that this latter scheme is exactly that used in [1,2]. However, it must be noticed that the resolved variable, obtained with such discretization, is not the deconvolved velocity $\tilde{u}$ but the one defined by the numeric resolution obtained on the mesh size h. All the coefficients of these schemes are reported in [3] and these discretizations then completed by the fourth order accurate second derivative for the diffusion term in (3).

3. SGS models for the LES equation

The first focus point to be highlighted is that if one performs a well-resolved DNS then in (3) one has $\tau \to 0$ (since $\lim_{\Delta\to 0} \tilde{u} = u$) but, if an LES is performed, then the Burgers equation (3) must be still closed by specifying some approximation for the unknown SGS term $\frac{1}{\Delta}(A^{(m)}\frac{\tau}{2})_{x-\Delta/2}^{x+\Delta/2}$ in terms of the resolved velocity $\tilde{u}$. Now, starting from the classical static and dynamic eddy viscosity models through the recent deconvolution based ones, e.g. see [4–8], the adopted SGS models are briefly addressed.

The Smagorinsky eddy viscosity model approximate the stress according to

$$A^{(m)}\frac{\tau}{2} \cong -(C_s\overline{\Delta})^2\left|\frac{\partial \tilde{u}}{\partial x}\right|\frac{\partial \tilde{u}}{\partial x}, \tag{4}$$

where $\overline{\Delta}$ is a characteristic length and C_s is a constant to be properly tuned. It is well known that, thanks to the Germano identity, the constant in (4) can be determined in a dynamic way without any "ad hoc" tuning. The dynamic procedure can be simply extended also to the deconvolved Burgers Eq. (3). Indeed, by choosing a second characteristic length $\hat{\Delta} > \overline{\Delta}$ and by applying again a filtering of this width on to Eq. (3) one gets

$$\frac{\partial \hat{\tilde{u}}}{\partial t} = \frac{1}{\Delta}\left[A^{(m)}\left(-\frac{\widehat{\tilde{u}}^2}{2} - \frac{T}{2}\right)\right]_{x-\Delta/2}^{x+\Delta/2} + \frac{\partial}{\partial x}\left(\nu\frac{\partial \hat{\tilde{u}}}{\partial x}\right),$$

where $T = (\hat{\tau} - \widehat{\tilde{u}}^2 + \widehat{\tilde{u}^2})$ is the new exact SGS term for flow scales below $\hat{\Delta}$. The Germano identity writes now as

$$T - \hat{\tau} \equiv L = \widehat{\tilde{u}^2} - \widehat{\tilde{u}}^2 \tag{5}$$

therefore, according to (4), by modelling also the new SGS term as $A^{(m)}\frac{T}{2} \cong -(C_s\hat{\Delta})^2|\frac{\partial \hat{\tilde{u}}}{\partial x}|\frac{\partial \hat{\tilde{u}}}{\partial x}$, by extracting an average value of the constant (since it appears under filtering $\hat{\tau}$), one gets the expression for the constant to be determined during calculation. Similarly to the molecular diffusive term, central conservative fourth order discretization is adopted for the eddy viscosity models.

The other two adopted SGS models are not based on the eddy viscosity assumption but they are derived following the hypothesis of scale-similarity between the smallest of the resolved flow scales and the biggest of the unresolved ones. Two recently proposed models are used, the Generalized Scale-Similarity (GSS) [6] and the Approximate Deconvolution Model (ADM) [7]. Such models are based on to the same idea that $u \cong \tilde{u} = G_m^{-1} * \overline{u}$ is a better approximation of the behaviour of the smallest resolved scales acting across the filter width [5]. The main differences between the two models stay in the fact that the exact SGS term $u^2 - \overline{u}^2$ is approximated as $(G_m^{-1} * \overline{u})^2 - \overline{(G_m^{-1} * \overline{u})}^2$ in the GSS model and $(G_m^{-1} * \overline{u})^2 - \overline{u}^2$ in the ADM one.

Since in our FV approach the exact SGS term is $\tau = u^2 - \tilde{u}^2$, such models rewrites specifically for our deconvolution-based Burgers equation as

$$\tau \cong \tilde{u}^2 - \tilde{\tilde{u}}^2, \tag{6}$$

$$\tau \cong \tilde{u}^2 - \tilde{u}^2 = 0 \tag{7}$$

for the GSS and ADM models, respectively. Therefore, Eq. (3) with $\tau = 0$ expresses an LES equation for the deconvolved velocity with the ADM model.

These approximations are no longer true for the FD fifth order upwind as well as for the FD central discretization. Indeed, for these latter, the ADM and GSS models [6–8] applies to Eq. (1) and slightly differ from Eqs. (6), (7) since the LES equation writes as

$$\frac{\partial \overline{u}}{\partial t} + \frac{\partial f(\overline{u})}{\partial x} = \frac{\partial \vartheta/2}{\partial x},$$

where the exact SGS term is $\vartheta = \bar{u}^2 - \overline{u^2}$. Therefore, according to the previous procedure $u \cong \tilde{u}$, the SGS modelling leads to

$$\vartheta \cong \bar{\tilde{u}}^2 - \overline{\tilde{u}^2}, \tag{8}$$

$$\vartheta \cong \bar{u}^2 - \overline{\tilde{u}^2} \tag{9}$$

for the GSS and ADM models, respectively.

4. Discussion of the results

The differential form of the Burgers equation is firstly solved in a DNS approach in order to build a database for comparison. However, the convective flux is recast and discretized in such a way to guarantee energy conservation in the inviscid limit, i.e.,

$$\alpha u \frac{\partial u}{\partial x} + \frac{(1-\alpha)}{2}\frac{\partial u^2}{\partial x},$$

with $\alpha = 1/3$. A classical fourth order central scheme (CE4) and a fourth order Runge–Kutta time integration have been implemented, the parameters of the simulation being $L = 1$, $\Delta t = 10^{-5}$, $\Delta_{\mathrm{DNS}} = 1/8192$, $\nu = 10^{-4}$. In such a way, the resolved field extends up to the Nyquist frequency $k_{\max} = 8192\pi$ and all the characteristic flow scales are well resolved as the cell Reynolds number is ensured to be no more than $O(1)$ during all the computation. The simulation is performed for the 32 samples and the averaged spectra are reported in Fig. 1(a) for different times. It can be seen that the inertial sub-range evolves toward the correct slope –2. Since the curves satisfying the differential equation $x'(t) = u(x(t), t)$ are the characteristic lines for the inviscid Burgers model, a visualization of the field dynamic in the x, t plane was obtained by constructing the iso-lines of the velocity field in such plane, see Figs. 1(b) and (c). Clearly, the coalescence of the curves indicates the formation of a high gradient (which becomes a singularity in the inviscid case) followed by the action that the molecular diffusion has on the evolution.

After having completed the DNS database, the computations were first performed (for all kind of discretization) with a no-model LES (or a coarse DNS), i.e. by setting $\tau = \vartheta = 0$, with the same parameters, but $\Delta_{\mathrm{LES}} = 8\Delta_{\mathrm{DNS}}$. However, in order for the SGS models effect to be then tested on a well-correlated velocity field, now the initial flow condition for LES was taken from the developed DNS field at $\bar{t} = 0.01$. The results obtained at $t_{\mathrm{LES}} = 0.01 = t_{\mathrm{DNS}} - \bar{t}$ are reported in Figs. 2(a)–(e). In order for a quantitative comparison to be obtained, the integral measure $\mathrm{NORMA} = \int_0^{\pi/\Delta_{\mathrm{LES}}} |(E_{\mathrm{DNS}} - E_{\mathrm{LES}})|\,\mathrm{d}k_q$ is also reported.

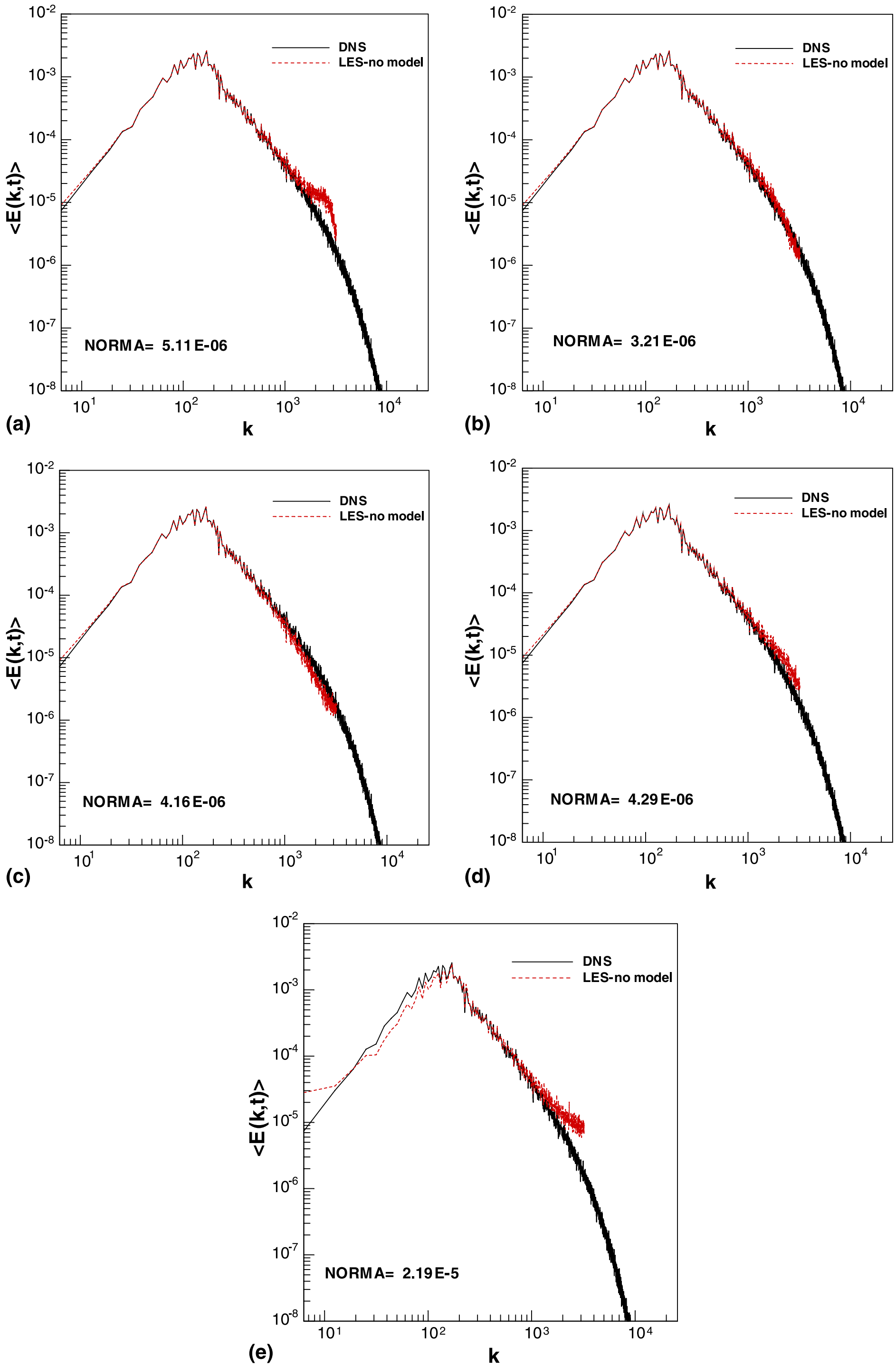

Fig. 2. LES no-model versus DNS: (a) CE4 scheme, (b) UW3 scheme, (c) UW5 scheme, (d) UWB5 scheme and (e) UWB5NC scheme.

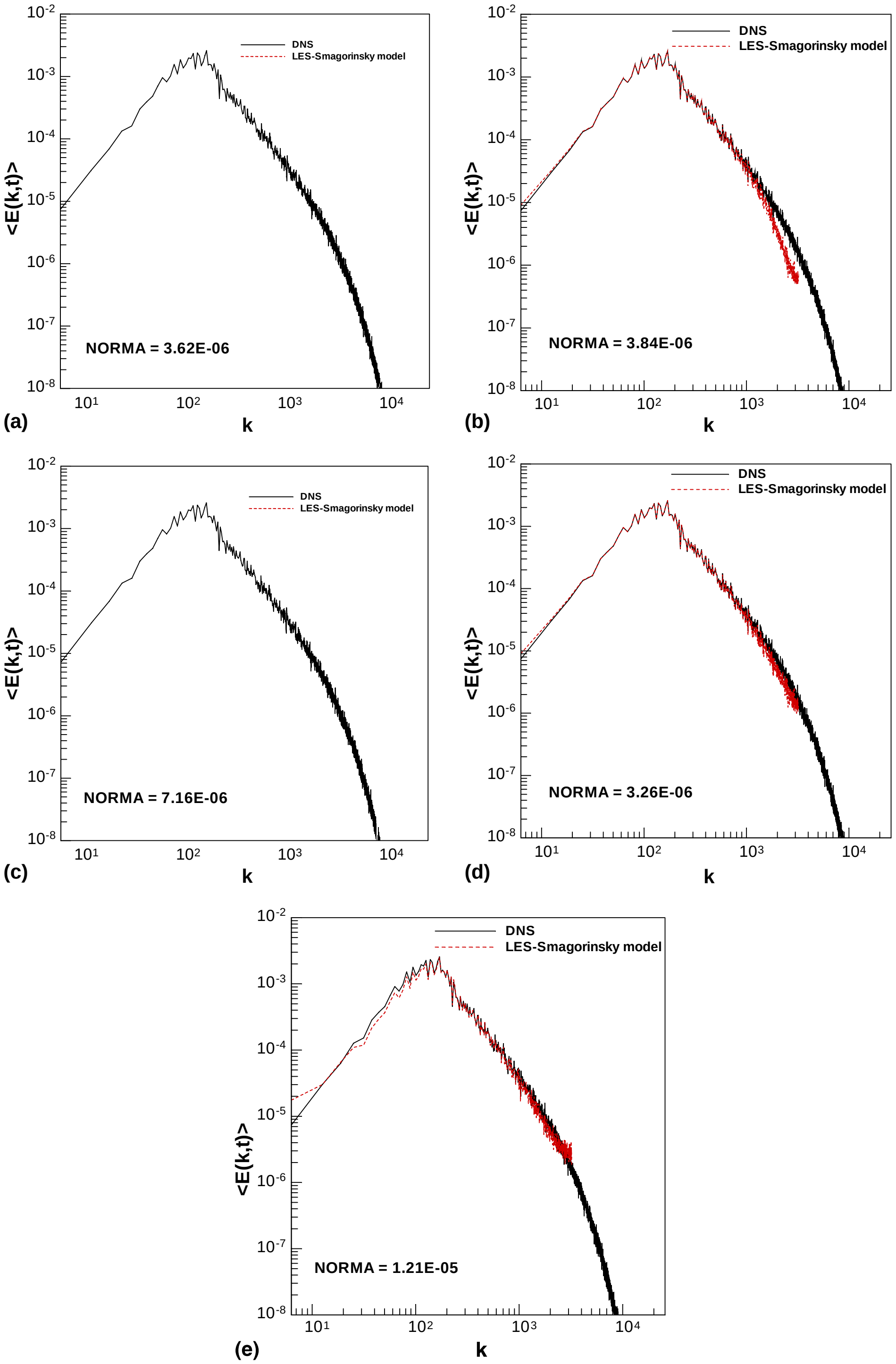

Fig. 3. LES with static Smagorinsky model versus DNS: (a) CE4 scheme, (b) UW3 scheme, (c) UW5 scheme, (d) UWB5 scheme and (e) UWB5NC scheme.

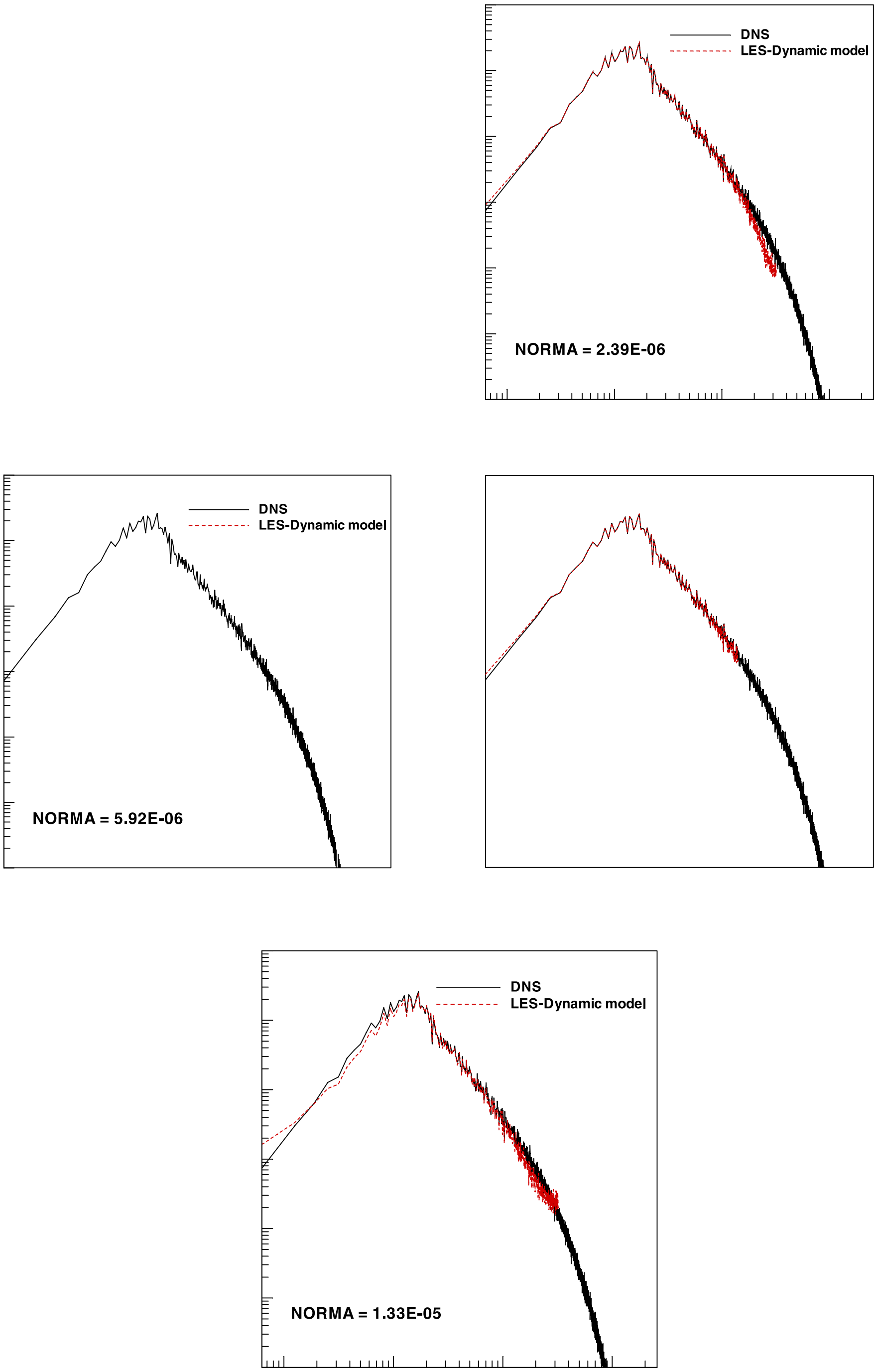

.mic Smagorinsky model versus DNS: (a) CE4 scheme, (b) UW3 scheme, (c) UW5 scheme, (d) UWB5 scheme .cheme.

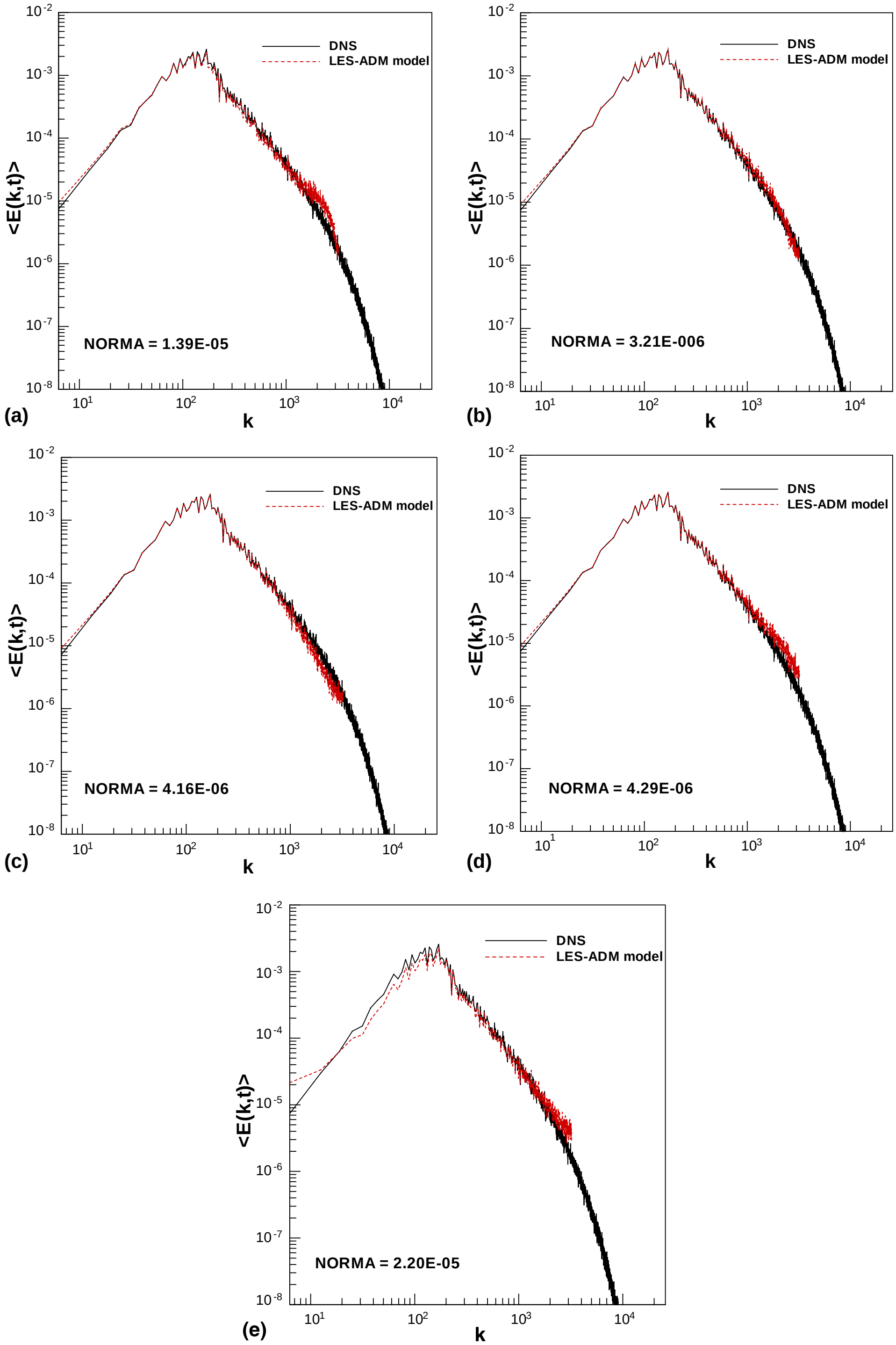

Fig. 5. LES with the ADM model versus DNS: (a) CE4 scheme, (b) UW3 scheme, (c) UW5 scheme, (d) UWB5 scheme and (e) UWB5NC scheme. Note that (b)–(d) are the same of Fig. 2.

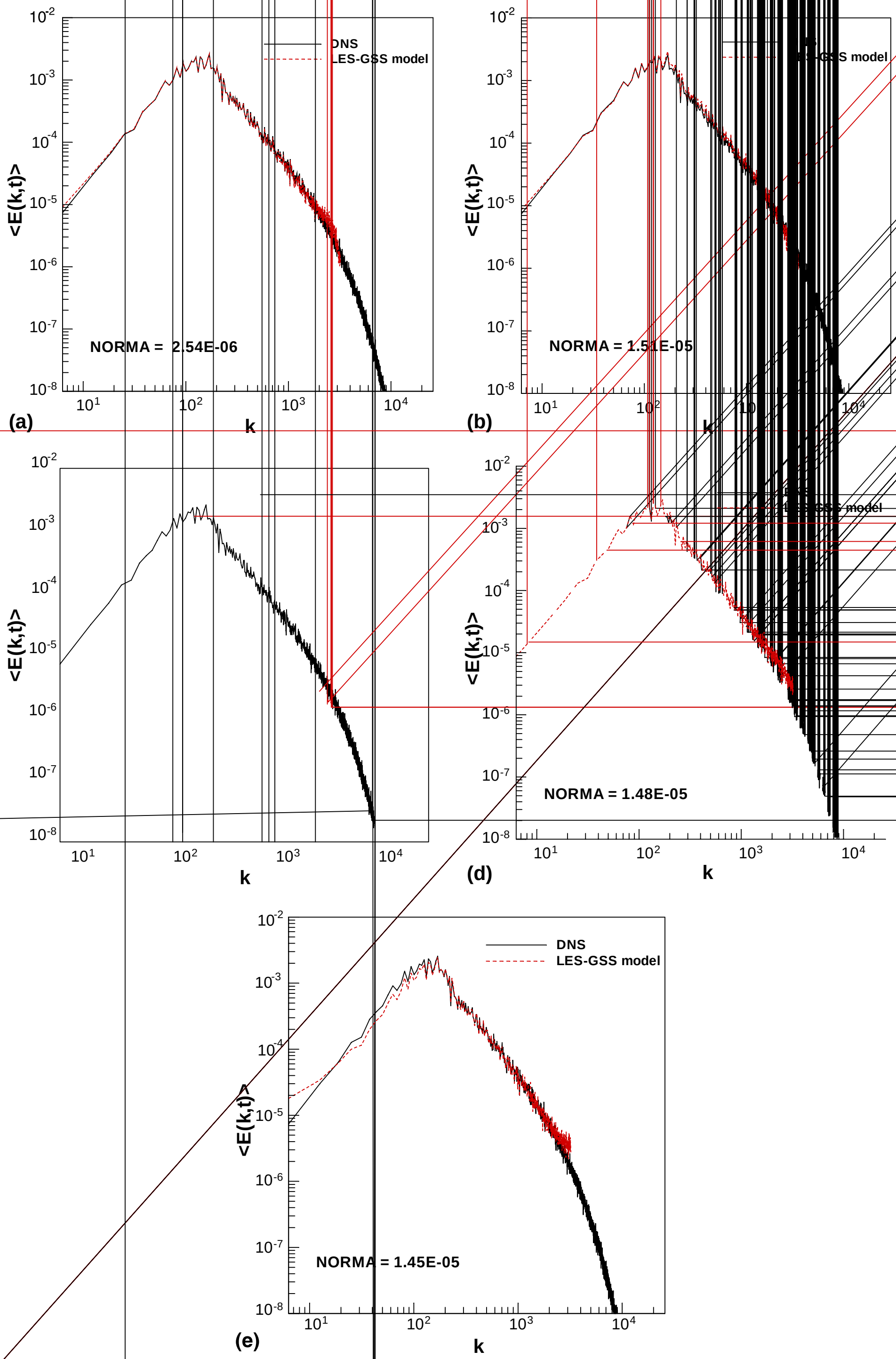

Fig. 6. LES with the GSS model versus DNS: (a) CE4 scheme, (b) UW3 scheme, (c) UW5 scheme, (d) UWB5 scheme and (e) UWB5NC scheme.

From the analysis of the figures, some conclusions can be already indicated. Despite the energy conservation property, the scheme CE4 shows the well known energy pile-up close the cut-off frequency $\pi/\Delta_{\mathrm{LES}} = 1024\pi$ that is a characteristic feature of its dispersion error. Thus, for such kind of discretization, an SGS model is expected to provide a sufficiently strong dissipation in order for the dispersive errors to be controlled. Eddy viscosity models seem to be opportune. Conversely, good results are obtained by using both UW3 and UW5 schemes, showing a well balanced effect between dispersive and dissipative contributions. It is expected that an optimal SGS model should be able not to alter such a balance, but only to guarantee inertial energy transfer. Owing to their high correlation, scale similarity models are supposed to be the most opportune. Slightly different is the result obtained for the UWB5 since the energy dissipation provided by the scheme seems to be not completely sufficient by alone. This result is someway opposite to the conclusion derived in [2], wherein a too strong dissipation was observed therefore the analysis of the UWB5NC is the key of lecture. Indeed, this is the worst result, where the energy spectrum is contaminated by numerical errors also at very low wavenumber. This feature was already observed and explained in [3], by deriving an analysis in Fourier space in terms of the modified coefficients d'_q of the numerical flux function, i.e.

$$\frac{1}{\Delta}\left[A^{(m)}\left(-\frac{\tilde{u}^2}{2}\right)\right]_{x_j-\Delta/2}^{x_j+\Delta/2} = \mathrm{i}\sum_q d'_q \mathrm{e}^{\mathrm{i}k_q\frac{L}{N}j}.$$

These coefficients (not real for upwind schemes) were compared with the exact one, i.e., the real coefficient $d_q = \frac{k_q}{2}\sum_{l+n=q}\hat{u}_l\hat{u}_n$ of the continuous flux function. It can be shown that, for FV conservative scheme, the modified coefficients have an imaginary part tending to zero for $k_q \to 0$ while the modified coefficient for the FD non-conservative form maintains a non-vanishing error along the imaginary axis (see [3]). Also according to the aliasing error discussion for FD schemes presented in [14], such effect can be now fully justified and it is expected that no SGS model can enhance this feature.

Finally, for the same Δ_{LES}, the LES results at t_{LES} with the (static and dynamic) Smagorinsky, ADM and GSS models are reported in Figs. 3–6, respectively. The value of the Smagorinsky constant is 0.2 for the

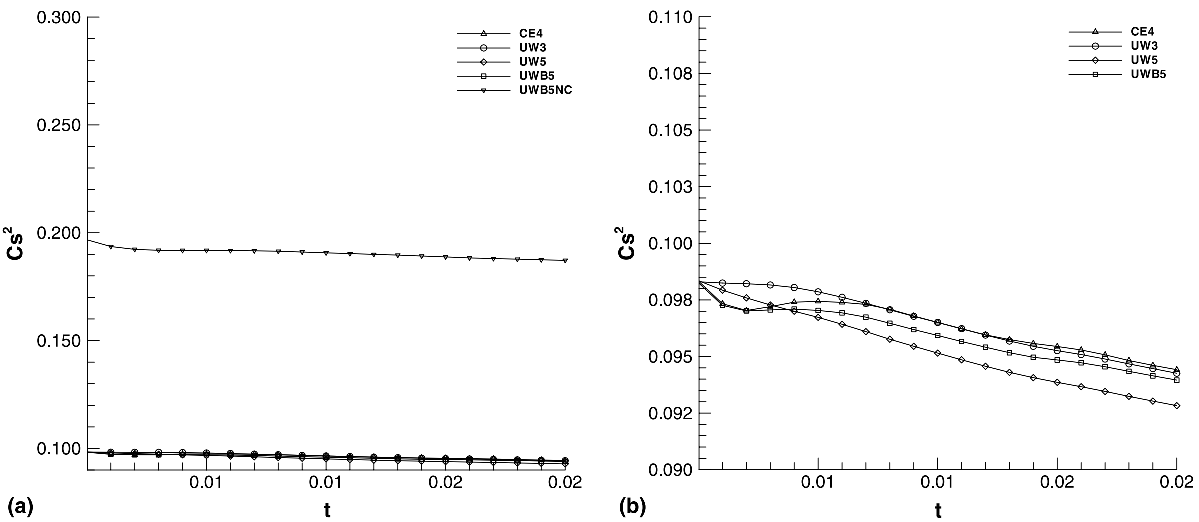

Fig. 7. (a) Time behaviour of $\langle C_s^2(t)\rangle$ for CE4, UW3, UW5, UWB5 and UWBNC5 schemes. (b) The same figure as (a) in a different scale.

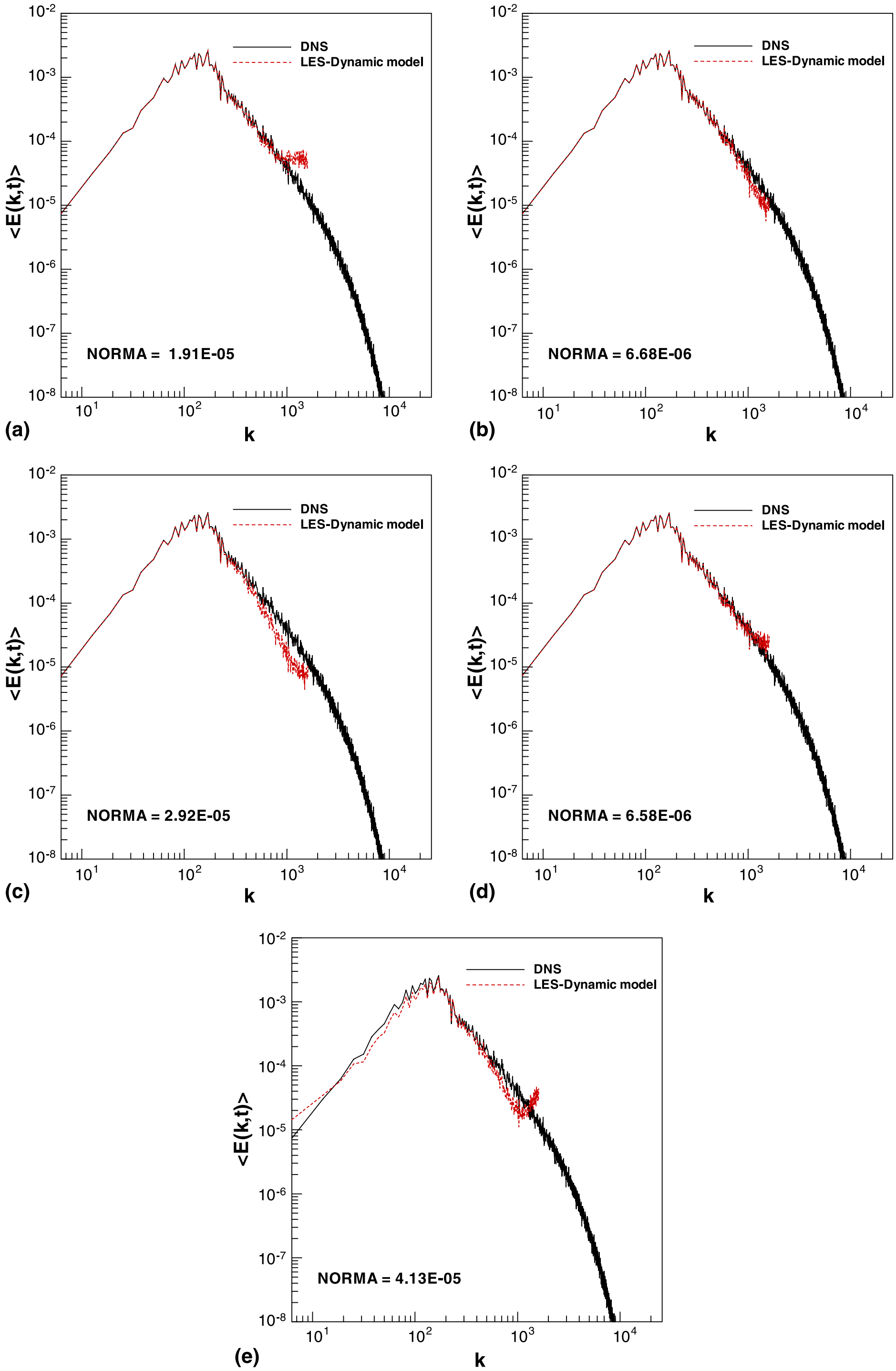

Fig. 8. Coarse LES with dynamic Smagorinsky model versus DNS: (a) CE4 scheme, (b) UW3 scheme, (c) UW5 scheme, (d) UWB5 scheme and (e) UWB5NC scheme.

static model while the characteristic length measure was $\overline{\Delta} = 2\Delta_{\mathrm{LES}}$. Such doubling has been chosen since the minimum resolvable wavelength is twice the mesh size. Consider also that the model approximates the $\tau/2$ term. On the other hand, the dynamic SGS model requires only a tuning of the value of the test-filter. The value $\hat{\Delta} = 4\overline{\Delta}$ was chosen. Discretization of derivatives in the SGS expression is centred and fourth order accurate.

From the analysis of the results it appears that good ones are obtained with the UW5B scheme practically for all cases whereas UW3 seems also good for ADM and GSS; CE4 gives very good results for all cases except ADM. However, the second deconvolution $\tilde{\tilde{u}}$ in the GSS model acts to slightly increase the resolved wavenumber components and a mixed GSS model seems to be indicated. Clearly, the eddy viscosity contribution smoothes the energy pile-up for the CE4 scheme, while altering the energy spectra for UW3 and UW5 schemes. Again, the solution with the UWB5NC appears always largely contaminated by numerical errors. An interesting feature to analyse is the time behaviour of the dynamic Smagorinsky constant. The ensemble average value is reported in Fig. 7 as function of time for the CE4, UW3, UW5, UWB5 and UWBNC5 schemes. Again, it appears that conservative FV upwind schemes require a contribution of the SGS model smaller than CE4 one, whereas a strong influence is required for the UWBNC5. As last result the LES with the dynamic Smagorinsky model are repeated by considering coarse grids, i.e., $\Delta_{\mathrm{LES}} = 16\Delta_{\mathrm{DNS}}$ and $\Delta_{\mathrm{LES}} = 32\Delta_{\mathrm{DNS}}$. The results obtained with the first grid are reported in Fig. 8 and confirm the good spectral resolution of the UWB5 scheme as well as the results obtained with the latter grids (for the sake of brevity the figures are not reported) that provided 1.08×10^{-4}, 8.73×10^{-5}, 1.51×10^{-4}, 8.45×10^{-5}, 2.14×10^{-4}, for the schemes CE4, UW3, UW5, UWB5, UWB5NC, respectively.

These results tell us that, according to [2], FD non-conservative upwind-biased schemes are not appropriate for performing LES. On the other hand, the results obtained with FV upwind schemes seem to indicate that the deconvolution technique alleviates the dissipative character of upwind discretization and provides good results in terms of spectral resolution. This feature is particularly interesting for LES methodology and in order for a clearer conclusion to be addressed on which is the best FV scheme, a real 3-D turbulent flow should be considered. Future studies on this issue appear necessary and, following [4], a simulation of a 3D channel flow is in progress.

References

[1] M.M. Rai, P. Moin, Direct simulation of turbulent flows using finite difference schemes, J. Comput. Phys. 109 (1991) 2.

[2] R. Mittal, P. Moin, Suitability of upwind-biased finite difference schemes for large eddy simulation of turbulent flows, AIAA J. 35 (8) (1997).

[3] G. De Stefano, F.M. Denaro, G. Riccardi, High order filtering formulation for control volumes simulation of turbulent flows, Int. J. Numer. Methods Fluids 37 (2001) 7.

[4] P. Iannelli, F.M. Denaro, G. De Stefano, A deconvolution-based fourth order finite volume method for incompressible flows on non-uniform grids, Int. J. Numer. Methods Fluids 43 (4) (2003) 431–462.

[5] P. Sagaut, Large Eddy Simulation for incompressible flows. An introduction, Springer, 2001.

[6] B.J. Geurts, Inverse modeling for large-eddy simulation, Phys. Fluids 9 (12) (1997).

[7] S. Stolz, N.A. Adams, An approximate deconvolution procedure for large-eddy simulation, Phys. Fluids 11 (7) (1999).

[8] N.A. Adams, S. Stolz, A subgrid-scale deconvolution approach for shock capturing, J. Comput. Phys. 178 (2002).

[9] J.M. Burgers, A mathematical model illustrating the theory of turbulence, Adv. Appl. Mech. 1 (1948).

[10] M.D. Love, Subgrid modelling studies with Burgers' equation, J. Fluid Mech. 100 (1980).

[11] A. Das, R. Moser, Optimal large-eddy simulation of forced Burgers equation, Phys. Fluids 14 (2002) 14.

[12] G. De Stefano, O.V. Vasilyev, Sharp cut-off versus smooth filtering in large eddy simulation, Phys. Fluids 14 (2002) 1.

[13] G. De Stefano, F.M. Denaro, G. Riccardi, Applicazione di un filtro di ordine elevato all'equazione di Burgers, AIMETA, 1999.

[14] A.G. Kravchenko, P. Moin, On the effect of numerical errors in Large Eddy Simulations of turbulent flows, J. Comput. Phys. 131 (1997).